Mechanical damping in instrumented impact testing

ÁKOS BEZERÉDI*‡, GYÖRGY VÖRÖS*§, BÉLA PUKÁNSZKY*‡
* *Technical University of Budapest, Department of Plastics and Rubber Technology, H-1521 Budapest, PO Box 92, Hungary*
‡ *Central Research Institute for Chemistry, Hungarian Academy of Sciences, H-1525 Budapest, PO Box 17, Hungary*
§ *Eötvös University Budapest, Institute for General Physics, H-1445 Budapest, PO Box 323, Hungary*

Instrumented impact testing is an effective tool for the study of high-speed fracture of polymeric materials. The evaluation of force signals is usually impeded by dynamic effects. These can be compensated by mechanical damping which, however, leads to additional energy absorption. A model and a technique were developed for the determination of the viscoelastic properties of the damper. Correction of the force versus deflection traces obtained in the instrumented impact test is carried out automatically during the evaluation of the test. Unbiased force versus deflection correlations are recovered and the most important fracture parameters are determined. Comparison of different correction techniques has shown the validity of the method. The agreement between K_c values calculated from the maximum force and fracture energy proved to be excellent. The developed technique greatly facilitates the evaluation of instrumented impact tests and increases the reliability of the measurement.

1. Introduction

Impact testing is of great practical importance in most applications of plastics, which lead to the development of standard methods such as the Charpy and Izod tests and later to the introduction of linear elastic fracture mechanics (LEFM), yielding fracture characteristics independent of specimen size [1]. Application of fracture mechanics, however, has strict conditions on size, which must be respected and checked. Valid LEFM conditions can be verified by calculation or by instrumented impact testing [2]. Moreover, instrumentation of a traditional impact pendulum offers valuable information on the fracture process, on the type of the fracture and on the extent of plastic deformation [3]. Instrumented impact testing has become increasingly accepted and used [4–12].

Impact testing is usually carried out at a high (more than $1\,m\,s^{-1}$) speed. At these high rates, dynamic effects occur, which make the evaluation of the force versus deflection curves difficult, or even impossible [13–15]. Periodic variation in the measured force signal is caused by the bouncing of the specimen and by stress waves developed on first contact with the hammer. The problems caused by dynamic effects can be decreased or completely avoided by three techniques: reducing the rate of the test [13, 15–19], electronic filtering [18, 20, 21] and mechanical damping [2, 22–24]. Reducing the velocity of impact is an accepted route and a standard procedure is developed for impact testing at a rate of $1\,m\,sec^{-1}$ [25]. However, in practice, fracture properties are often measured at much higher rates [15, 18, 21, 26]. In such cases, dynamic effects are overwhelming. Electronic filtering is not recommended, because it alters the measured signal and leads to erroneous force values [3]. Mechanical damping is widely used to reduce dynamic effects: the presence of the damper leads to additional energy losses and the need for a correction [25].

The goal of our study was to investigate the effect of mechanical damping in an instrumented impact test and to develop a technique for the correction of energy losses introduced by the presence of the damper. Determination and quantitative description of the viscoelastic properties of the damper make possible the exact calculation of the original load versus time traces and the determination of the most important fracture characteristics, K_c and G_c.

2. Mechanical damping

In Fig. 1 the force measured during the fracture of a specimen is presented as a function of time. The measurement was carried out without any damping or filtering. The specimen dimensions were $63\,mm \times 10\,mm \times 4\,mm$, the span of the supports 40 mm and the rate of fracture $2.9\,m\,s^{-1}$. The length of the notch was 1.5 mm. The polypropylene sample studied contained 0.1 volume fraction of $CaCO_3$ filler. Under these conditions the oscillation of the measured force

0022–2461

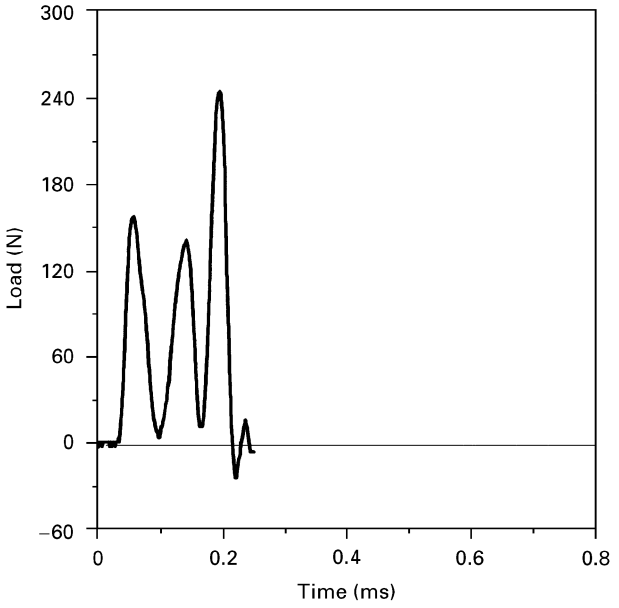

Figure 1 Load versus time curve measured in instrumented impact testing without damping or filtering.

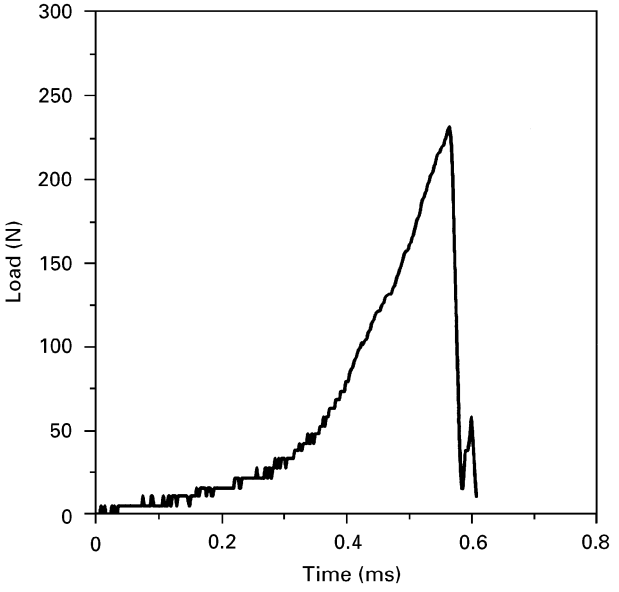

Figure 2 Load versus time curve of the same material as in Fig. 1, but measured with mechanical damping.

signal is very strong; determination of the maximum force or the absorbed energy is almost impossible.

The use of a silicone rubber damper of 1.5 mm thickness results in a completely different load versus time trace (Fig. 2). Oscillation of the force signal is absent and the most important characteristics, i.e., the maximum force, time to fracture, slope and absorbed energy, can be easily determined. However, the trace shows additional features due to damping. Force builds up gradually during fracture; the time to fracture is considerably longer than without the damper (compare with Fig. 1). Fig. 2 can be converted into a force versus displacement correlation (Fig. 3); the area under the first part of the curve corresponds to the energy absorbed by the rubber, which is comparable with the energy used for the fracture of the specimen. This part must be deducted from the total energy measured, in order to obtain the true fracture properties of the sample. Moreover, the maximum force used

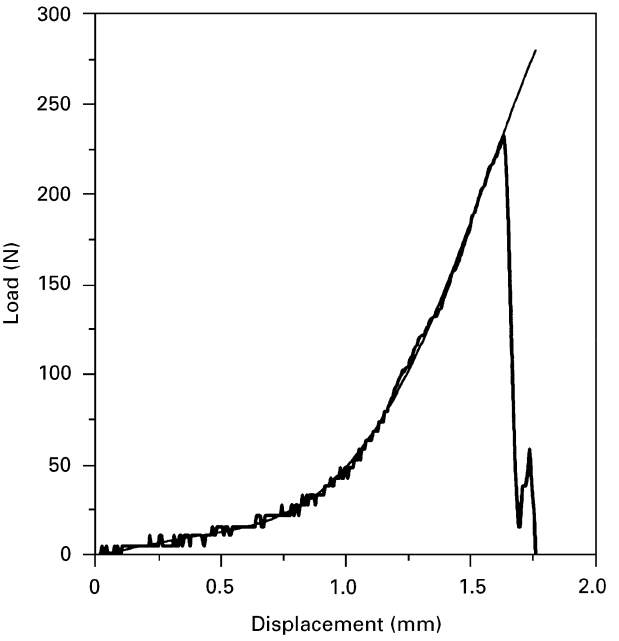

Figure 3 Fig. 2 transformed into a load versus displacement correlation. (——), fitted polynomial (Equation 21).

for the calculation of K_c might be biased as well, leading to erroneous values.

The energy absorbed by the damper depends on numerous factors, on its viscoelastic properties, on the thickness, on the rate and extent of deformation, etc. The most diverse materials are used as the damper: putty [22, 24], silicone grease [2, 25], or different elastomers and rubbers [23]. Highly viscous pastes must be administered to the specimen in a uniform thickness. Homogeneity and constant thickness are vital for reliable measurement and reproducibility. The disadvantage of this technique is that each specimen has to be treated separately and the energy correction is carried out with a specimen and a damper, which are different form those used in the actual fracture test. Elastomers, on the other hand, are glued to the tup and can be used in many experiments. Homogeneity of the damper is very important also in this case, as well as its complete recovery after fracture.

After trying several elastomers we have chosen a silicone rubber for our experiments. The elastomer was compression moulded into sheets of different thicknesses (0.5, 1.0, 1.5 and 2.0 mm) at 180 °C for 15 min and then cured at 200 °C for 4 h. Small, 3 mm × 15 mm, strips glued to the tup were used in the damping experiments. None of the other elastomers tried was sufficiently homogeneous to use it as the damper. Homogeneity of the silicone rubber was checked by compression and rebound experiments. Standard deviation of energy absorption in compression was 2%, while, in the rebound test the maximum load and the time to maximum load showed deviations of 6% and 3%, respectively.

3. Determination of elastomer properties

In order to account for the additional energy absorption and to reproduce the original load versus

deformation trace, the viscoelastic properties of the damper must be determined and quantitatively described. To achieve this, model experiments were carried out which simulated the deformation of the rubber during fracture as closely as possible. At the beginning of the fracture process the damper deforms at a high rate, with the speed of the hammer. With increasing acceleration of the sample, the rate of deformation of the damper decreases. Close to fracture initiation the maximum deformation is reached; the rate of deformation becomes zero. In the further course of the measurement the elastomer relaxes and recovers its initial dimensions.

These conditions were modelled in rebound experiments. The damper was glued to the tup and a weight of the same size and shape as the fracture specimen was dropped onto it in a specially designed rig. The weight and drop height were chosen to give the initial deformation rate and similar maximum loads as those of the fracture test. A typical load versus time correlation is shown in Fig. 4, while the load versus deformation function derived from it is shown in Fig. 5. The damper consumes considerable energy represented by the area of the loop. Recovery is rather slow, but complete.

The simple model and the coordinate system chosen for the description of the deformation of the damper are presented in Fig. 6. The origin of the coordinate system is chosen at the surface of the tup, m is the mass of the weight, while ρ is the density and L the undeformed thickness of the damper. A is the contact surface between the two bodies and v_0 is the speed of the weight at the beginning of the deformation. During the deformation of the damper, the stress developing at a certain height x and time t is $\sigma(x, t)$, but we can measure only the force on the surface of the tup, which is

$$f(0, t) = A\sigma(0, t) \tag{1}$$

The correlation of the displacement field, $u(x, t)$, and the deformation, $\varepsilon(x, t)$, of the damper is given by

$$\varepsilon(x, t) = \frac{\partial u}{\partial x} \tag{2}$$

Deformation of the damper is given by the following wave equation [27] :

$$\rho \frac{\partial^2 u}{\partial t^2}(x, t) = \frac{\partial \sigma}{\partial x}(x, t) \tag{3}$$

which relates the deformation to the stress through as yet unknown constitutive equation. Equation 3 is associated with the following initial and boundary conditions:

$$u(0, t) = 0 \quad \dot{u}(L, 0) = -v_0 \tag{4}$$

During its deformation the damper is coupled to the mass dropped on it; this coupling is expressed by

$$m \frac{\partial^2 u}{\partial t^2}(L, t) = -A\sigma(L, t) \tag{5}$$

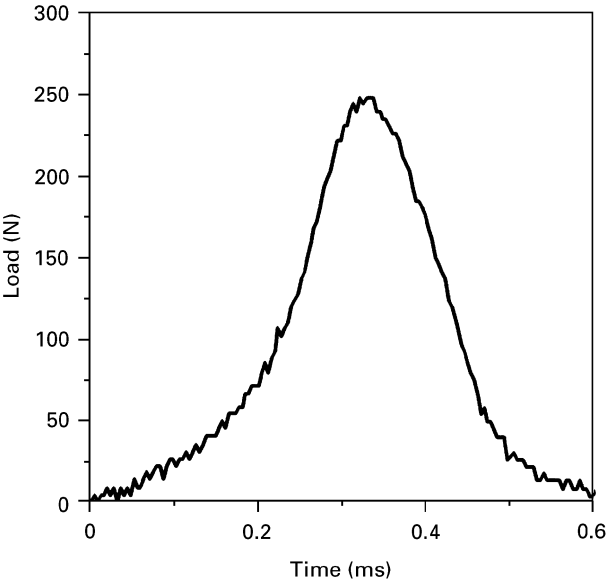

Figure 4 Load versus time trace measured in a rebound test on a silicone rubber damper.

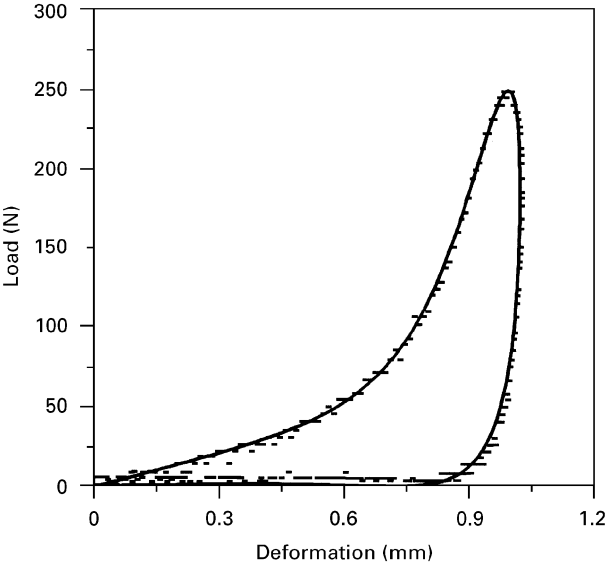

Figure 5 The correlation of Fig. 4 transformed into a load versus deformation curve. (—), theoretical fit (Equation 18).

We assume that the constitutive equation of the damper depends not only on the deformation but also on the deformation rate, i.e.,

$$\sigma = \sigma(\varepsilon, \dot{\varepsilon}, \varepsilon^2, \dot{\varepsilon}^2, \cdots) \tag{6}$$

One of the most important conditions for the validity of this treatment is the existence of homogeneous deformation in the elastomer. Force is measured on the surface of the tup, i.e., at $x = 0$, both in the model experiment and during fracture. If the damper does not deform homogeneously, the actual force related to the deformation and fracture of the specimen cannot be determined. As a consequence, the first step of our analysis must be the verification of the existence of homogeneous stress in the damper. In order to do this, acceleration is expressed from Equation 3 and introduced into the boundary condition of

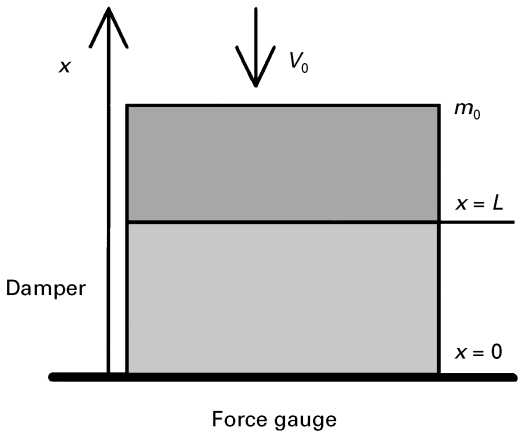

Figure 6 Model and coordinate system of a rebound test.

Equation 5:

$$\frac{m}{\rho}\frac{\partial\sigma(L,t)}{\partial x} = -A\sigma(L,t) \tag{7}$$

The stress function, $\sigma(x, t)$, obtained from the solution of the wave equation is expanded into a Taylor series according to the x coordinate, i.e.,

$$\sigma(x,t) = c_0(t) + c_1(t)x + c_2(t)x^2 + \cdots \tag{8}$$

where $c_0, c_1, c_2, \ldots$ are the coefficients of the series, while the gradient of the stress is expressed as

$$\frac{\partial\sigma(x,t)}{\partial x} = c_1(t) + 2c_2(t)x + 3c_3(t)x^2 + \cdots \tag{9}$$

Equations 8 and 9 are introduced into Equation 7, which is then rearranged into the following form:

$$\frac{c_1(t) + 2c_2(t)L + 3c_3(t)L^2 + \cdots}{c_0(t) + c_1(t)L + c_2(t)L^2 + \cdots} = -\frac{A\rho}{m} \tag{10}$$

Both sides of Equation 10 are multiplied by L in order to express its right-hand side in a dimensionless form, i.e.,

$$\frac{c_1(t)L + 2c_2(t)L^2 + 3c_3(t)L^3 + \cdots}{c_0(t) + c_1(t)L + c_2(t)L^2 + \cdots} = -\frac{A\rho L}{m} \tag{11}$$

On the right-hand side of Equation 11, $A\rho$L corresponds to the mass of the damper, while m corresponds to that of the weight dropped onto it. Taking into consideration the actual conditions of the test, the ratio of the two masses is a very small value, close to zero (less than 10^{-2}). The left-hand side of Equation 11 satisfies the equality at each moment only in the case when

$$c_0(t) \gg c_1(t)L + 2c_2(t)L^2 + 3c_3(t)L^3 \ldots \tag{12}$$

However, this inequality indicates that the first term dominates in the series expressed by Equation 8, i.e., it equals with good approximation

$$\sigma(x,t) \approx c_0(t) \tag{13}$$

The result obtained and represented by Equation 13 unambiguously proves the homogeneity of stresses in the damper. According to the constitutive equation (Equation 6) also ε and $\dot{\varepsilon}$ are homogeneous, if the above condition is fulfilled, i.e., stress is independent of x. In this case we can write that

$$\sigma(L,t) = \sigma(x,t) = \sigma(0,t) \tag{14}$$

Thus the equation of motion of the weight dropped on the damper takes the following form:

$$m\ddot{u}(L,t) = -A\sigma(0,t) = -f(0,t) \tag{15}$$

and the displacement, deformation and deformation rate of the damper are expressed as

$$y(x) = y(L)\frac{x}{L}$$

$$\varepsilon = \varphi(t)\frac{y(L)}{L} \propto u(L,t)$$

$$\dot{\varepsilon} = \dot{\varphi}(t)\frac{y(L)}{L} \propto \dot{u}(L,t) \tag{16}$$

Since the damper proved to be homogeneous the constitutive equation can be written as

$$f(0,t) = f[u(L,t),\ \dot{u}(L,t) + \cdots] \tag{17}$$

The next step of the analysis is the determination of the actual form of the constitutive equation. Knowing the values of the mass, m, the initial rate, v_0, and the force, $f(t)$, measured during the rebound test, the integration of this latter by time leads to $u(t)$, and the $\dot{u}(t)$ functions. As a consequence, the force versus displacement correlation describing the deformation of the damper can be obtained (Fig. 5). Owing to the large deformation and high deformation rate, the deformation of the damper cannot be described by a linear viscoelastic model. We have found that the load versus deformation correlation presented in Fig. 5 can be described well by the following constitutive equation:

$$f = \dot{u}a_1[\exp(a_2u) - 1] + a_3[\exp(a_4u) - 1] + a_5\dot{u}^2u \tag{18}$$

where $a_1, \ldots, a_5$ are constants characterizing the damper. Equation 18 describes the deformation of a non-linear anelastic body, which cannot be modelled by the usual linear viscoelastic elements, i.e., Hook elastic springs and Newtonian dashpots. The model resembles a Voigt–Kelvin body containing deformation-dependent components according to Fig. 7. The viscoelastic properties of the elements are given by the following expressions:

$$\eta_1 = a_1[\exp(a_2t) - 1] \quad \eta_2 = a_5\dot{\varepsilon}\varepsilon$$

$$E = a_3[\exp(a_4t) - 1] \tag{19}$$

The two parallel dashpots cannot be replaced by a single element since the viscosity of one depends on deformation, but that of the other depends on both deformation and deformation rate. The a_i parameters are determined by the least-squares technique from

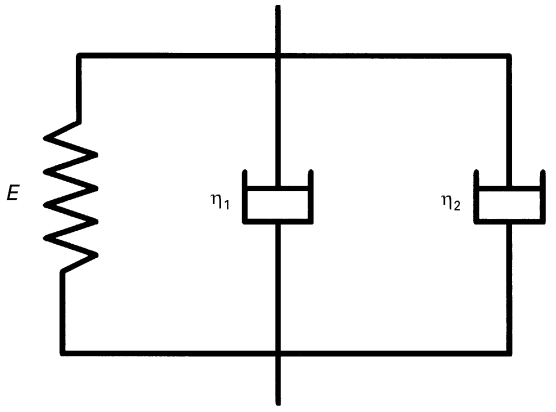

Figure 7 Non-linear viscoleastic model of the damper.

the measured $f(t_i)$ and the calculated $u(t_i)$; the $u(t_i)$ expressions are given according to

$$S = \sum_{i=1}^{N} \{ f(t_i) - \dot{u}a_1[\exp(a_2 u) - 1] - a_3[\exp(a_4 u) - 1] - a_5 \dot{u}^2 u \}^2 \qquad (20)$$

The calculated force versus deformation correlation is represented by a solid curve in Fig. 5. The agreement between the correlation calculated from the measured values and the model is extremely good; thus the developed constitutive equation can be used for energy correction in instrumented impact testing carried out with mechanical damping.

4. Evaluation of fracture measurements: correction

In an instrumented impact test the force developing during the deformation and fracture of a specimen is measured as a function of time. Displacement of the three components of the system, i.e., the hammer, the specimen and the damper, is not known. Calculation of the deformation of the damper is the most difficult task, but now it can be done with the help of the constitutive equation. We know $f(t)$ and the solution of Equation 18 gives the displacement of the damper. Since the equation is complicated, the solution cannot be given in a closed form; it must be solved numerically. We assume that the displacement of the damper can be described by the following polynomial expression:

$$u_d(t) = v_0 t + \sum_{i=1}^{5} b_i t^{i+1} \qquad (21)$$

where v_0 is the initial speed of the hammer at the beginning of the test. Our experience has shown that the use of a sixth-order polynomial is sufficient for the description of the displacement, u_d. The polynomial fitted to the force versus displacement trace is represented by a straight line in Fig. 3. The value of the b_i parameters is determined by variation calculation and they are selected to satisfy Equation 18.

If we know the displacement of the damper, those of the hammer and the specimen can be calculated. The

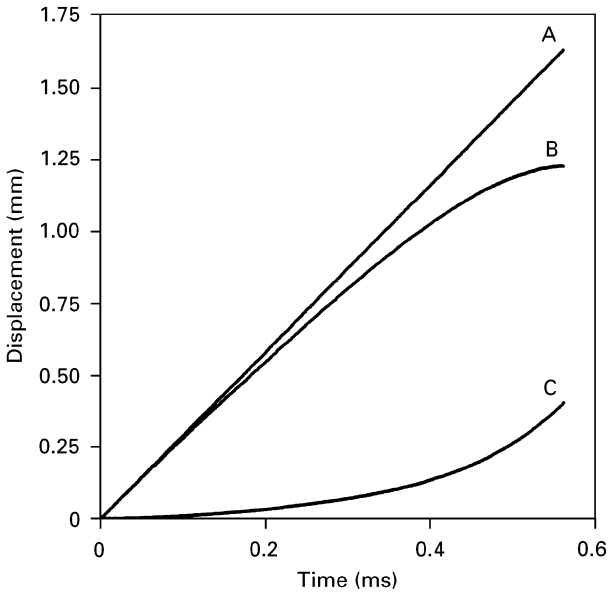

Figure 8 Displacement of the components in an instrumented impact test with mechanical damping. Curve A, hammer; curve B, damper; curve C, specimen.

displacement of the hammer is determined as usual, i.e.,

$$u_h(t) = v_0 t - \frac{1}{M} \int_0^t \int_0^{t'} f(t'') \, dt'' \, dt_0 \qquad (22)$$

where M is the mass of the hammer. Displacement of the specimen is given by

$$u_s(t) = u_h(t) - u_d(t) \qquad (23)$$

Compression of the damper and the displacement of the hammer, as well as that of the specimen are shown in Fig. 8. The displacement of the hammer is almost linear, as expected, but those of the damper and the specimen are non-linear. Compression of the damper is a maximum at around fracture initiation, where the measured force also reaches a maximum value. Deformation rate of the damper decreases continuously and reaches zero at this point (Fig. 9), verifying our earlier assumption.

From the measured force and the calculated displacements the real force versus deflection curve of the specimen can be reconstructed. The corrected trace is presented in Fig. 10. Only the first part of the correlation changed (see Fig. 3); the maximum force, however, remained untouched, i.e., dynamic stress intensity factors are not changed by mechanical damping. Comparison of Figs 3 and 10 shows that deformation of the damper makes up a major part of the total deformation in the studied case of the mechanical damping. Correction of the force versus deformation correlation allows us to determine all the relevant parameters necessary for the fracture characterization of any material, i.e., the maximum force, the specimen deflection, and the energy consumed by fracture. This latter can be calculated from

$$U_s = \int f(t) \, du_h(t) - \int f(t) \, du_d(t) \qquad (24)$$

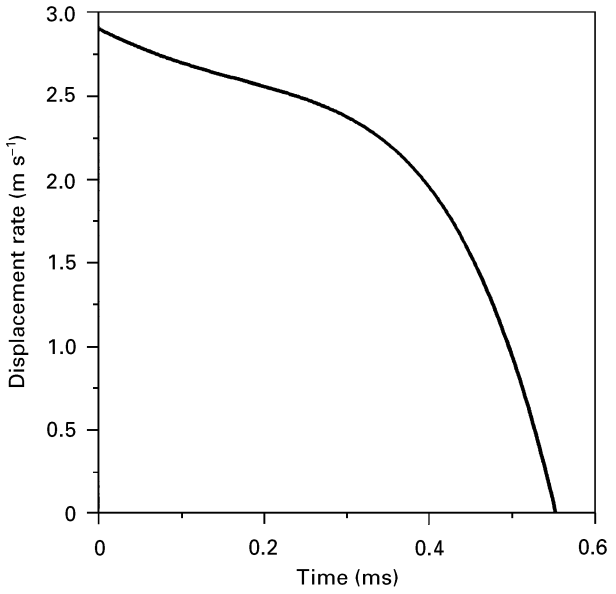

Figure 9 Changes in the displacement rate, $\dot{u}(L,\ t)$, of the damper during the impact test.

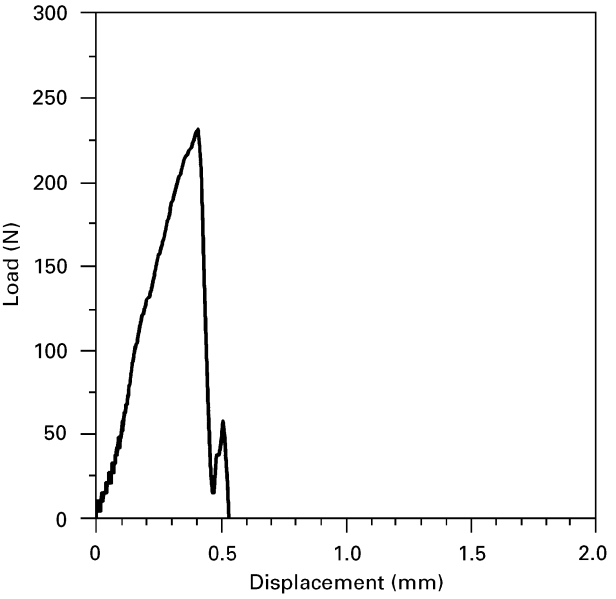

Figure 10 The correlation of Fig. 3 corrected by the deformation of the damper.

5. Application: comparison of corrections

The dynamic fracture resistance of polymers is characterized by the critical stress intensity factor, K_c, and the critical strain energy release rate, G_c, determined from the energy consumed during fracture. K_c can be calculated from the force measured at fracture initiation (maximum force or 5% offset from the initial slope, P) by

$$K_c = \psi \frac{P}{BD^{1/2}} \tag{25}$$

where ψ is a parameter depending on the compliance of the specimen, B is the width of the specimen and D is the thickness of the specimen. We saw that damping does not influence the value of the maximum force; thus correction is not necessary here. Mechanical damping, however, greatly facilitates the determination of P, since in the absence of dynamic effects its determination is easy and accurate. The value of K_c was 2.08 MPa m$^{1/2}$ for the material used in this study.

G_c, on the other hand, is determined from the energy consumed during fracture. There are, however, several energy-consuming processes in a fracture experiment, i.e., the total energy, U_T^2, measured can be divided into the following most important components:

$$U_T = U_f + U_{ind} + U_{kin} + U_d \tag{26}$$

where U_f is the energy used for the fracture of the specimen, U_{ind} is the indentation energy due to compliance of the specimen and the machine, U_{kin} is the kinetic energy and U_d is the energy consumed by the damper. Correction for kinetic energy loss is not necessary, since it does not depend on the length of the notch; thus it does not influence the value of G_c. Indentation must be corrected in all cases, and also in measurements when mechanical damping is not used. Naturally, U_d must be taken into account if damping is applied.

An often-used technique for the calculation of U_T is to fit a straight line to the linear part of the force versus time curve and to integrate the area up to maximum force [14, 28]. This procedure can be used in the case of brittle fracture, but K_c and G_c can be calculated only under valid LEFM conditions anyway. In the case of mechanical damping, this technique leads to erroneous values, since the slope of the straight part of the curve also depends on the properties of the damper. This becomes obvious if we compare the slopes of the damped and corrected force versus displacement traces presented in Figs 3 and 10. Moreover, a linear part of the curve is often difficult to define or does not exist at all.

The effect of mechanical damping is usually corrected in a separate experiment. The hammer or weight is dropped on the fully supported damper with the same velocity as in a fracture test but, because of the full support, fracture does not take place. The hammer is stopped by a limiter to avoid damage of the transducer. Correction is carried out by integrating the obtained force versus displacement correlation up to the maximum force measured in the actual fracture test and deducting the energy obtained from U_T. This technique assumes constant deformation rate of the damper during fracture. It has been shown, however, that this assumption is not true and the rate of deformation drops to zero at the initiation of fracture (see Fig. 9). The energy calculated by this technique and the actual energy consumed by the damper, therefore, can differ significantly.

The effect of mechanical damping can be corrected by taking into account the viscoelastic properties of the damper as presented above. The difference between the two techniques is demonstrated in Fig. 11. The area, P, under the two curves integrated up to the maximum force gives the correction term in both cases. It is obvious that the constant-rate experiment

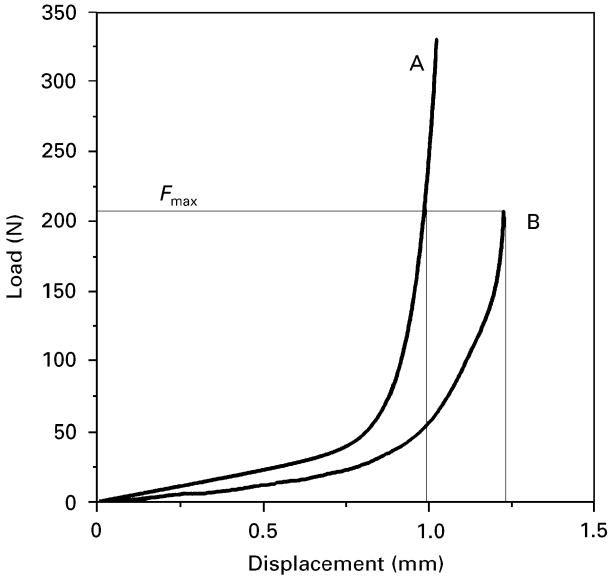

Figure 11 Energy correction. Curve A, constant rate; curve B, viscoelastic analysis.

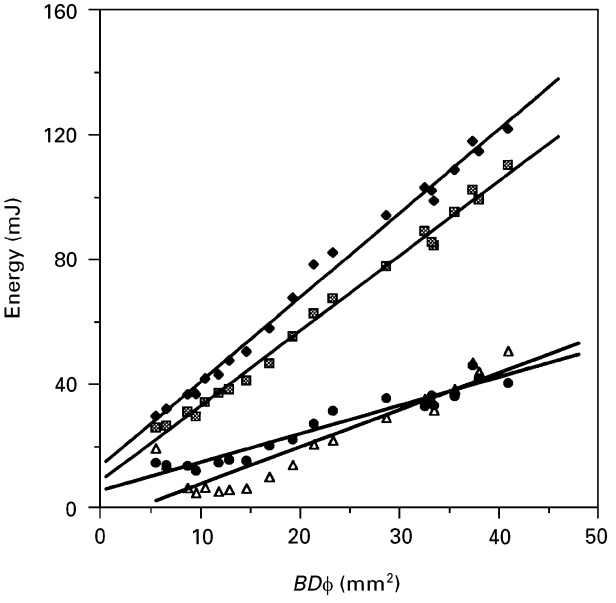

Figure 12 Determination of strain energy release rate from U versus $BD\phi$ plots. (◆), without correction; (▩), linear fit; (△), constant rate; (●), viscoleastic analysis.

underestimates the energy consumed by the damper. Correction for indentation and damping can also be carried out simultaneously.

G_c is determined from the measured energy by plotting it as a function of $BD\phi$, where ϕ is a geometric factor, which can be calculated or taken from tables. The strain energy release rate is given by the slope of the linear plot. Different calculation and correction techniques are compared in Fig. 12. Straight lines are obtained in all cases, but the slopes (and thus the G_c values) differ considerably. The numerical data are listed in Table I together with K_c values calculated from G_c with the well-known correlation for plane-strain conditions:

$$K_c^2 = \frac{G_c E}{1 - \nu^2} \tag{27}$$

TABLE I Dynamic fracture properties of the studied material obtained by different techniques and corrections (see also Fig. 12)

Property (units)	Method or correction			
	Without correction	Linear fit	Constant rate	Viscoelastic analysis
G_c (kJ m^{-2})	2.61	2.33	1.20	0.83
K_c (MPa m$^{1/2}$)	3.48	3.41	2.45	2.04

The difference between the non-corrected and corrected G_c values is large and can amount to more than 300%. The agreement between the K_c value obtained from the maximum load (2.08 MPa m$^{1/2}$) and from G_c (2.04 MPa m$^{1/2}$) is best when both the indentation and the viscoelastic correction are used, which further supports the validity of our approach.

6. Conclusions

It was shown that the best technique for the compensation of dynamic effects in instrumented impact testing is the application of mechanical damping. The additional energy consumed by the damper must be taken into account when the fracture characteristics are calculated. The technique developed for this correction takes into account the viscoelastic properties of the damper and determines them quantitatively by the numerical calculation of the parameters of the constitutive equation of the damper. The software developed for the correction carries out all calculations automatically. The use of the technique was justified and its validity verified by the good agreement between the measured and calculated force versus deformation functions, by the obtained deformation and rate of deformation functions of the damper and by the similarity of the K_c values calculated from the maximum load and G_c. The technique was experimented and verified for a silicone rubber damper. Further experiments must be carried out with dampers of very diverse viscoelastic properties such as putty, silicone grease and other elastomers. Attention must be paid also to the fact that the energy correction was significant in the case studied; it was necessary to correct the energy by 70% in order to obtain G_c. The effect of damper thickness on G_c must also be studied in the future down to a very small or even zero thickness.

Acknowledgements

The authors are indebted to Wacker Chemie GmbH for supplying the silicone elastomer. The technical assistance of Tauril Gumigyártó és Kereskedelmi kft. is acknowledged as well as the useful advice and suggestions of Professor J.G. Williams. The authors are grateful for financial support from the National Scientific Research Fund of Hungary (Grants T 016500, T 017637 and F 016085) which made possible the research on instrumented impact testing of polymeric materials.

References

1. J. G. WILLIAMS, "Fracture mechanics of polymers" (Ellis Horwood, Chichester, West Sussex, 1984).
2. T. CASIRAGHI, G. CASTIGLIONI and T. RONCHETTI, *J. Mater. Sci.* **23** (1988) 459.
3. T. CASIRAGHI, *Polym. Engng Sci.* **18** (1978) 833.
4. P. J. HOGG, *Compos. Sci. Technol.* **29** (1987) 89.
5. A. GOLOVOY, *Polym. Engng Sci.* **25** (1985) 903.
6. G. LEVITA, A. MARCHETTI and A. LAZZERI, *Polym. Compos.* **10** (1989) 39.
7. M. BRAMUZZO, *Polym. Engng Sci.* **29** (1989) 1077.
8. M. AKAY and D. BARKLEY, *Polym. Testing* **7** (1987) 391.
9. R. S. J. CORRAN, R. A. W. MINES and C. RUIZ, *Int. J. Fract.* **23** (1983) 129.
10. P. ZOLLER, *Polym. Testing* **3** (1983) 197.
11. F. MARTINATTI and T. RICCO, *J. Mater. Sci.* **29** (1994) 442.
12. J. M. HODGKINSON, *Polym. Prepr.* **29** (1988) 143.
13. W. BÖHME and J.F. KALTHOFF, *Int. J. Fract.* **20** (1982) 139.
14. A.P. GLOVER, F.A. JOHNSON, J.C. RADON and C.E. TURNER, in proceedings of the International Conference on Dynamic Fracture Toughness, London, 5–7 July 1976 (Welding Institute, American Society of Metals; 1976) pp. 63–75.
15. G. C. ADAMS, R. G. BENDER, B. A. CROUCH and J. G. WILLIAMS, *Polym. Engng Sci.* **30** (1990) 241.
16. M. BRAMUZZO, A. SAVADORI and D. BACCI, *Polym. Compos.* **6** (1985) 1.
17. C. B. BUCKNALL, *Pure Appl. Chem.* **58** (1986) 985.
18. D.R. IRELAND, Proceedings of the Internationsl Conference on Dynamic Fracture Toughness, London, 5–7 July 1976 (Welding Institute, American Society of Metals, 1976) pp. 47–62.
19. D. M. BIGG and E. J. BRADBURY, *Polym. Engng Sci.* **32** (1992) 287.
20. D. R. IRELAND, in "Instrumented impact testing", edited by T.S. DeSisto (American Society for Testing and Materials, Philadelphia, PA, 1974) p. 3.
21. D. BARKLEY and M. AKAY, *Polym. Testing* **11** (1992) 249.
22. J. G. WILLIAMS, "Fracture mechanics of polymers" (Ellis Horwood, Chichester, West Sussex, 1984) p. 242.
23. N. J. MILLS and P. S. ZHANG, *J. Mater. Sci.* **24** (1989) 2099.
24. T. VU-KHANH and J. M. CHARRIER, in Proceedings of the Symposium on the Quantum Character of Plastics and Rubber, (1984) p. 1.
25. A. PAVAN, "High rate K_e and G_c testing of plastics", ESIS TC 4 recommendation for impact testing of plastics.
26. T. VU-KHANH and B. FISA, *Polym. Compos.* **7** (1986) 375.
27. L.D. LANDAU and E.M. LIFSCHITZ, "Theory of elasticity" (Pergamon, London, 1959).
28. H. HOFFMANN, W. GRELLMANN and V. ZILVAR, in "Polymer composites", edited by B. Sedláček (Walter de Gruyter, Berlin, 1986) p. 233.

Received 8 December 1995
and accepted 30 July 1997